Published in final edited form as:
J Hepatol. 2011 April ; 54(4): 765–772. doi:10.1016/j.jhep.2010.09.039.

Glycogen Synthase Kinase-3 (GSK-3) Inhibition Attenuates Hepatocyte Lipoapoptosis

Samar H. Ibrahim[1], **Yuko Akazawa**[3], **Sophie C. Cazanave**[1], **Steven F. Bronk**[1], **Nafisa A. Elmi**[1], **Nathan W. Werneburg**[1], **Daniel D. Billadeau**[2], and **Gregory J. Gores**[1]

[1] Division of Gastroenterology and Hepatology, College of Medicine, 200 First Street SW Rochester, MN, 55905, USA

[2] Division of Oncology Research Mayo Clinic, College of Medicine, 200 First Street SW Rochester, MN, 55905, USA

[3] Department of Internal Medicine, Nagasaki University School of Medicine, Nagasaki 852-8562, Japan

Abstract

BACKGROUNDS AND AIMS—Saturated free fatty acids induce hepatocyte lipoapoptosis, a key pathologic feature of nonalcoholic steatohepatitis. The saturated free fatty acid palmitate induces hepatocyte lipoapoptosis via an endoplasmic reticulum stress pathway resulting in c-Jun-N-terminal (JNK) activation. Glycogen synthase kinase (GSK)-3 is a serine/threonine kinase which may also promote JNK activation. Thus our aim was to determine if GSK-3 inhibition suppresses palmitate induced JNK activation and lipoapoptosis.

METHODS—We employed mouse primary hepatocytes, Huh-7 and Hep3B cell lines for these studies.

RESULTS—Palmitate-induced GSK-3 activation was identified by phosphorylation of its substrate glycogen synthase. GSK-3 pharmacologic inhibition, by GSK-3 inhibitor IX and enzastaurin, significantly reduced PA-mediated lipoapoptosis. More importantly, Huh-7 cells in which either GSK-3α or GSK-3β isoforms were stably and selectively knocked down by shRNA displayed resistance to palmitate-induced cytotoxicity. GSK-3 pharmacological inhibitors and shRNA-targeted knockdown of GSK-3α or GSK-3β also suppressed JNK activation by palmitate. JNK activation, in part, promotes lipoapotosis by inducing expression of the pro-apoptotic effector p53-upregulated modulator of apoptosis (PUMA). Consistent with this concept, GSK-3 pharmacologic inhibition also reduced PUMA cellular protein levels during exposure to palmitate. On the other hand, the GSK-3 inhibitors did not prevent PA induction of ER stress.

In **CONCLUSION,** our results suggest GSK-3 activation promotes a JNK-dependent cytotoxic signaling cascade culminating in lipoapoptosis.

Address for correspondence: Gregory J. Gores, MD, Professor of Medicine, Mayo Clinic College of Medicine, 200 First Street SW, Rochester, Minnesota 55905, Tel: 507 284 0686, Fax: 507 284 0762, gores.gregory@mayo.edu.

Disclosure: The authors have no potential conflict of interest in regards to this manuscript.

Keywords

endoplasmic reticulum stress; glycogen synthase kinase; JNK; lipoapoptosis; nonalcoholic steatohepatitis; PUMA

INTRODUCTION

Nonalcoholic fatty liver disease (NAFLD) is an emerging public health problem linked to the increased incidence of obesity, insulin resistance and overt diabetes [1]. Up to 30% of the population is afflicted by NAFLD [2] and a subset of these patients develops nonalcoholic steatohepatitis (NASH). Individuals with NASH can progress to cirrhosis with its sequelae including the development of portal hypertension, end-stage liver disease and hepatocellular carcinoma [3]. Thus, the cellular and molecular mechanisms promoting liver injury in NASH are of biomedical and public health interest.

Obesity and insulin resistance are associated with increased circulating levels of non-esterified or free fatty acids (FFA), which are disproportionately increased in NASH as compared to NAFLD [4]. FFAs are taken up in the liver where they are esterified into neutral triglycerides. However, an excess of FFA is deleterious for the liver. Indeed, saturated FFAs are directly hepatotoxic, in part, by promoting apoptosis, which in this context is referred to as lipoapoptosis [5,6]. The importance of this process in human disease is highlighted by observations that hepatocyte lipoapoptosis and serum biomarkers of this pathologic process correlate with NASH severity [7,8]. Saturated FFA are more toxic than unsaturated FFA, presumably given their ability to disrupt endoplasmic reticulum (ER) homeostasis causing an ER stress response [9]. Biosensors of ER stress include protein kinase RNA-like ER kinase (PERK) and inositol-requiring protein-1α (IRE-1α). These two resident transmembrane-ER proteins sense and transduce the ER stress response [10]. PERK activation drives the expression of the transcription factor C/EBP-homologous protein (CHOP) [11,12]. CHOP in turn increases expression of Growth Arrest and DNA Damage Protein 34 (GADD34). PERK dimerization also results in inactivating phosphorylation of elongation initiation factor 2α (eIF2α), thereby limiting protein synthesis. On the other hand GADD34 promotes protein synthesis by dephosphorylating eIF2α, shutting down the unfolded protein response and exacerbating the ER stress [11]. IRE-1α possesses endonuclease activity for *XBP-1* mRNA, creating a spliced form of *XBP-1*, the resultant spliced *XBP-1* mRNA via transcriptional activity promotes degradation of misfolded ER glycoproteins [10,13].

We and others have reported that FFA-induced ER stress is associated with c-Jun-N-terminal kinase (JNK) activation, which has been well documented in both rodent and human steatohepatitis [14–17]. ER stress-associated JNK activation promotes apoptosis by modifying expression and function of pro-apoptotic members of the Bcl-2 family, especially the Bcl-2 homology 3 (BH3) only protein Bcl-2-interacting mediator of cell death (Bim) and p53-upregulated modulator of apoptosis (PUMA) [18,19]. During lipotoxicity, JNK appears to promote apoptosis predominantly by inducing expression of PUMA. As we have previously reported, JNK inhibition reduces PA-induced increases of PUMA expression [18], and protects against PA induced apoptosis [14]; also PUMA knockdown by shRNA markedly reduces lipoapoptosis [18]. On the other hand, JNK inhibition does not prevent PA-induced Bim protein induction/activation during lipoapoptosis [20]. However, the precise cellular and molecular mechanisms resulting in JNK activation have not been fully elucidated, and mechanistic insight into this process may identify therapeutic targets to treat human NASH.

Glycogen synthase kinase (GSK)-3α and GSK-3β are serine/threonine kinases which can participate in pro-apoptotic signaling [21–24]. These kinases share 84% overall identity and 98% homology in their catalytic domains [25]. The mechanisms governing their respective and unique activation remain unclear. However, several studies have identified GSK-3 activation during ER stress [26–28]. For example, pharmacologic inhibition of GSK-3 attenuates ER stress-induced apoptosis in neuroblastoma cells, neurons and fibroblasts [29,30]. Moreover, GSK-3 is capable of activating JNK directly and GSK-3 activation of JNK contributes to an acute model of liver injury by acetaminophen [24]. Given this information, a potential role for GSK-3 in FFA-associated ER stress mediated JNK activation warrants exploration.

MATERIALS AND METHODS

Cell lines, cell isolation, and transfection

The human hepatocellular carcinoma cell lines, Huh-7, and Hep3B cells were cultured in Dulbecco's modified Eagle's medium (DMEM) as previously described [31]. Mouse hepatocytes were isolated from C57/Bl6 wild type mice by collagenase perfusion, purified by Percoll gradient, and cultured in Waymouth Medium [32]. Huh-7 cells were transfected separately with 1 μg/ml DNA plasmid (GSK-3α or GSK-3β MISSION short hairpin (sh) RNA lentiviral plasmid; Sigma Aldrich) using Lipofectamine (Invitrogen, Carlsbad, CA). Stably transfected GSK-3α and GSK-3β clones were selected in medium containing 1200 mg/liter G418 and screened by immunoblot analysis.

Fatty acid treatment

Palmitate (PA) (# P5585) was obtained from Sigma-Aldrich (St. Louis, MO). PA was dissolved in isopropanol at a concentration of 160 mM. PA was added to DMEM containing 1% bovine serum albumin to obtain a physiologic ratio between bound and unbound FFA in the media [33]. The concentration of PA used in the experiments varied between 400–800 μM and are similar to the fasting total FFA plasma concentrations observed in human with non-alcoholic steatohepatitis [4,34].

Quantification of apoptosis, Bax activation and mitochondrial membrane potential (MMP) Assay

Apoptosis was quantified by evaluating the characteristic nuclear changes of apoptosis using the nuclear binding dye DAPI (Molecular Probes, Eugene, OR) and fluorescence microscopy (Zeiss LSM 510, Carl Zeiss, Jena, Germany)[14]. Caspase 3/7 activation in cell lines was measured using Apo-ONE homogeneous caspase 3/7 kit (Promega, Madison, WI) according to the manufacturer's instructions [14]. Immunocytochemistry for active confirmation of Bax was performed using mouse anti-universal Bax (clone 6A7,1:100 dilution, Santa Cruz) as previously described by us in detail [18]. Huh 7 cells were cultured on glass-bottom plates (MatTek, Ashland, MA) and treated with reagents for 18 hours. The mitochondrial membrane potential was quantified as previously described by us in detail [35].

Real time polymerase chain reaction (PCR)

Real time PCR was performed as previously discussed by us [20] using the following primers: human PUMA, forward 5′-GACGACCTCAACGCACAGTA-3′ and reverse 5′-AGGAGTCCCATGATGAGATTGT-3′, size 101 bp; human CHOP, forward 5′-ATGGCAGCTGAGTCATTGCCTTTC-3′ and reverse 5′-AGAAGCAGGGTCAAGAGTGGTGAA-3′, size 177 bp; and human GADD34 forward 5′-CGACTGCAAAGGCGGC-3′ and reverse 5′-CAGGAAATGGACAGTGACCTTC-3′, size

107 bp. As internal control, primers for 18S ribosomal RNA (rRNA) were used: forward 5′-CGTTCTTAGTTGGTGGAGCG-3′ reverse 5′-CGCTGAGCCAGTCAGTGTAG-3′, size 212 bp

Detection of XBP-1 splicing

Human XBP-1 cDNA encompassing the region of PstI restriction site was amplified using the following primers: forward 5′-AAACAGAGTAGCAGCTCAGACTGC-3′ and reverse 5′-TCCTTCTGGGTAGACCTCTGGGAG-3′. The PCR products were then digested with PstI restriction enzyme (Biolabs, catalog #R0140) for 1 hour at 37°C, and subjected to 1.5% agarose gel electrophoresis; the gels were photographed under UV transillumination as previously described by us in detail [31]. Thapsigargin (TG) was used as an established inducer of XBP-1 splicing [9].

Immunoblot analysis

Whole cell lysates were prepared and subjected to immunoblot analysis as previously described [20]. Samples containing 50 μg proteins were resolved by 10–15% SDS-PAGE, transferred to nitrocellulose membranes, and incubated with primary antibodies at a dilution of 1:1000. Membranes were incubated with appropriate horseradish peroxidase-conjugated secondary antibodies (Biosource International, Camarillo, CA) at a dilution of 1:3000. Bound antibody was visualized using chemiluminescent substrate (ECL, Amersham, Arlington Heights, IL) and was exposed to Kodak X-OMAT film (Eastman Kodak, Rochester, NY).

Antibodies and Reagents

Rabbit anti-JNK (#9252), rabbit anti-phospho-JNK (Thr183/Tyr185) (# 9251), rabbit anti-Phospho-eIF2α (Ser51) (#9721), rabbit anti-eIF2α (#9722), rabbit anti-GSK-3α (#9338), rabbit anti-GSK-3β (#9315) and rabbit anti-phospho-glycogen synthase antibody (Ser649) (#3891) were from Cell Signaling Technology (Beverly, MA). Rabbit anti-PUMA was from Abcam (Cambridge, MA). Goat anti-β-actin was from Santa Cruz Biotechnology (Inc., Santa Cruz, CA). GSK-3 inhibitor IX (GSK IX) (#361550) and thapsigargin (#586005) were from Calbiochem (San Diego, CA). Z-VD(OMe)VAD(OMe)-FMK (ZVAD) was from MP Biomedicals (Aurora, Ohio). Enzastaurin (Enz) was provided by Lilly (Indianapolis, Indiana). BSA, Bradford reagent, and all other chemicals were from Sigma Aldrich.

Statistical analysis

All data represent at least three independent experiments and are expressed as means ± SE. Differences between groups were compared using Student's *t* tests and one-way analysis of variance with *post hoc* Dunnett test, and p values <0.05 were considered statistically significant.

RESULTS

GSK-3 inhibitor attenuates Palmitate-mediated lipoapoptosis

Initially we examined the effect of GSK-3α and GSK-3β inhibition on PA-mediated lipoapoptosis in Huh-7 cells. The GSK IX [36] and enzastaurin (a bisindolylmaleimide serine threonine kinase inhibitor that inhibits protein kinase C and GSK-3 [37]) were employed to inhibit both GSK-3α and GSK-3β. We confirmed that PA stimulated GSK-3, and the inhibitors effectively reduced PA-induced GSK-3 activity by assessing phosphorylation of glycogen synthase, a specific GSK-3 substrate. Following PA treatment, glycogen synthase phosphorylation was identified by phospho immunoblot analysis which was reduced by both inhibitors (Fig. 1A). The inhibitors also reduced PA-mediated

cytotoxicity in a concentration-dependent manner, each with a maximal inhibition at 2 μM (Fig. 1B). Because caspase 3/7 activation mediates the apoptotic phenotype, we next confirmed that the observed apoptosis was caspase-mediated. Indeed, PA-induced apoptosis was caspase-dependent, as it was reduced by the caspase inhibitor ZVAD (Fig. 1C, 1D). Both GSK-3 inhibitors also reduced apoptosis as assessed by this biochemical parameter (Fig. 1E). The GSK-3α and GSK-3β inhibitor IX also reduced caspase 3/7 activity in Hep3B cells and primary murine hepatocytes (Fig. 1F, 1G). Finally to exclude off-target effect of the pharmacologic inhibitor, apoptosis was examined in Huh-7 cells, in which GSK-3α or GSK-3β had been reduced by shRNA technology (Fig. 2A). Importantly, the knockdown of either GSK-3α or GSK-3β reduced PA-induced lipoapoptosis as assessed by both morphological and biochemical criteria (Fig. 2B, 2C).

Activation of Bax, a known mediator of mitochondrial dysfunction, is required for induction of hepatocyte lipoapoptosis downstream of JNK and BH3-only proteins activation [14,18]. Activated Bax was identified by immunofluorescence using the 6A7 monoclonal antibody which detects an active Bax conformation [38]. As previously reported, Bax activation was observed in PA-treated cells [14], but this activation was decreased when cells were treated with PA plus GSK IX (Fig. 3A). Likewise, selective shRNA targeted knockdown of either GSK-3α or GSK-3β, also reduced PA-induced Bax activation (Fig. 3B). Along with Bax activation, mitochondrial dysfunction with loss of mitochondrial membrane permeability (MMP) is a prominent feature of the mitochondrial pathway of apoptosis. The MMP was reduced to 39 ± 3% of the control value following treatment with PA; in contrast the MMP was maintained with the addition of the GSK-3 inhibitor (Fig 3C). Taken together, these data indicate that GSK-3α and GSK-3β pharmacologic or genetic inhibition potently suppresses saturated FFA cytotoxicity. Both isoforms appear to contribute to cytotoxicity by PA suggesting cooperation between the isoforms during lipoapoptosis. Given that GSK-3 inhibitor cytoprotection was similar in cell lines and primary mouse hepatocytes, we employed the Huh-7 cell line for subsequent studies to further elucidate the role of GSK-3 in lipotoxicity.

GSK-3 activation is downstream of ER stress-induced Lipoapoptosis

Lipoapoptosis can be attenuated downstream or upstream of FFA-induced ER stress [14,18,20,31,39]; therefore, we sought to determine if GSK-3 inhibition modulated PA-mediated ER stress. However, the pharmacologic inhibitors GSK-3 IX and enzastaurin did not prevent *CHOP* mRNA expression (Fig. 4A). GSK IX also did not prevent *GADD34* mRNA expression (Fig. 4B), or eIF2α phosphorylation (Fig. 4C) by PA, all indices of PERK activation. Likewise, GSK IX did not block *XBP-1* mRNA splicing (Fig. 4D), an indicator of IRE-1α activation. Collectively these data suggest that GSK-3 inhibition attenuates PA-induced lipoapoptosis downstream of ER Stress.

GSK-3 inhibition reduces JNK activation and PUMA upregulation during treatment with PA

Interestingly, activating JNK phosphorylation by PA was significantly reduced in the presence of the GSK IX (Fig. 5A) or enzastaurin (data not shown). Consistent with the pharmacologic inhibition, knockdown of GSK-3α or GSK-3β also attenuated JNK activation by palmitate (Fig. 5B). Consistent with this observation, GSK IX or enzastaurin also effectively attenuate upregulation of *PUMA* mRNA expression by PA (Fig. 6A). GSK IX was effective in reducing PA-induced PUMA expression at the protein level (Fig. 6B). However GSK IX did not reduce JNK activation by thapsigargin (Fig. 5C). These results suggest that GSK-3 inhibition may inhibit PA- mediated cell death through inhibition of JNK and reduction of the associated increase of PUMA.

DISCUSSION

Results of the present study provide mechanistic insights regarding the pro-apoptotic effects of GSK-3 during FFA-induced lipoapoptosis. The principal findings of this study indicate that during PA-mediated lipoapotosis in vitro: i) either pharmacological or genetic inhibition of GSK-3 attenuates apoptosis; ii) GSK-3 inhibition does not reduce the ER stress response; and iii) GSK-3 inhibition attenuates JNK activation, and subsequent PUMA induction. Each of these results is discussed in greater details below.

GSK-3 is a serine/threonine protein kinase with two isoforms (α and β). Both isoforms are ubiquitously expressed in cells and tissues, and have similar, although, not identical biochemical properties [25]. However, they are not interchangeable functionally, as demonstrated by the embryonic-lethal phenotype observed when the gene that encodes GSK-3β was knocked out [40]. Although GSK-3 has multiple functions in health, in the context of cytotoxic stimuli, GSK-3 (especially GSK-3β) appears to function as a pro-apoptotic kinase [41]. Previous studies have suggested that GSK-3β promotes the mitochondrial pathway of apoptosis through phosphorylation of Bax thereby facilitating its mitochondrial translocation [21]. More recently GSK-3β was also reported to activate JNK in acetaminophen-induced liver injury [24]. These prior studies have focused on GSK-3β rendering the role of GSK-3α in apoptosis ambiguous [42]. Our current study extends these observations by suggesting that both GSK-3 isoforms contribute to lipoapoptosis. Indeed, shRNA targeted knockdown of either GSK-3 isoform was protective against lipoapoptosis. The two isoforms apparently have complementary, non redundant roles in this model of apoptosis. The mechanisms by which these two isoforms cooperate in lipoapoptosis will require further detailed study.

Lipoapoptosis can be inhibited either upstream or downstream of ER stress. Although GSK-3 inhibition has been reported to reduce ER stress [28], in our current study the PA-induced ER stress response was not repressed by GSK-3 inhibition. These observations indicate that GSK-3 inhibition likely attenuates lipoapoptosis downstream of ER stress; however, we can not exclude a non ER stress-dependent pathway of GSK-3 activation. How GSK-3 is activated is not clear. Several studies suggest GSK-3 is activated by protein phosphatase 2A (PP2A) [43,44], GSK-3β is also known to be activated by PP2A during ceramide induced apoptosis [45]. Moreover, we have previously reported that PP2A activity was stimulated by saturated free fatty acids in hepatocytes during lipoapotosis [20]. Thus, PP2A activation is a potential mechanism contributing to GSK-3 stimulation during lipoapoptosis.

Activated JNK is an important downstream mediator of ER stress-associated lipoapoptosis and it has been implicated in human and murine steatohepatitis [15–18]. Several studies have suggested that GSK-3β is involved in JNK activation through interaction with upstream kinases such as mitogen-activated protein kinase/extracellular signal-regulated kinase kinase kinase (MAPKKK) and mixed lineage kinase (MLK) in neuronal and kidney cell lines [46,47]. GSK-3 was also reported to cooperate with JNK for the execution of the c-Jun stress response and neuronal death in response to trophic deprivation [22]. We note that in our present study, GSK-3 inhibition reduced PA-induced JNK phosphorylation, but it did not inhibit JNK phosphorylation in response to thapsigargin-induced ER stress. These data indicate that GSK-3 inhibition is not a general inhibitor of ER stress-associated JNK activation, but rather specifically antagonizes JNK activation by cytotoxic FFA.

The current study demonstrates that GSK-3 inhibition attenuates JNK-dependent dysregulation of PUMA, a key pro-apoptotic protein. PUMA promotes Bax activation and the mitochondrial pathway of cell death (Fig. 7). Activated Bax induces mitochondrial outer

membrane permeabilization (MOMP) which leads to the egress of these pro-apoptotic mediators into the cytosol. Subsequently, these mediators help activate downstream effectors caspases culminating in the apoptotic phenotype [48]. Collectively, our study suggests that GSK-3 genetic or pharmacologic inhibition attenuates saturated FFA-induced cell death in hepatocytes by inhibiting JNK-mediated PUMA upregulation. Given this mechanistic insight, we speculate that GSK-3 inhibition could have a potential therapeutic role in human NAFLD.

Acknowledgments

Grants: This work was supported by NIH Grants DK41876 to GJG, P50 CA102701 to DDB, the Optical Microscopy Core of P30 DK 84567, and the Mayo Foundation.

Abbreviations

NAFLD	nonalcoholic fatty liver disease
NASH	nonalcoholic steatohepatitis
FFA	free fatty acids
ER	endoplasmic reticulum
PERK	protein kinase RNA-like ER kinase
IRE-1α	inositol-requiring protein-1α
CHOP	C/EBP-homologous protein
GADD34	growth arrest and DNA damage protein 34
eIF2α	elongation initiation factor 2α
JNK	c-Jun-N-terminal kinase
BH3	Bcl-2 homology 3
Bim	Bcl-2-interacting mediator of cell death
PUMA	p53-upregulated modulator of apoptosis
GSK	glycogen synthase kinase
PA	palmitate
MMP	mitochondrial membrane potential
sh	short hairpin
PCR	polymerase chain reaction
TG	thapsigargin
GSK IX	GSK-3 inhibitor IX
ZVAD	Z-VD(OMe)VAD(OMe)-FMK
Enz	enzastaurin
PP2A	protein phosphatase 2A
Veh	vehicle
WT	wild type

References

1. Parekh S, Anania FA. Abnormal lipid and glucose metabolism in obesity: implications for nonalcoholic fatty liver disease. Gastroenterology. 2007; 132(6):2191–207. [PubMed: 17498512]
2. Browning JD, et al. Prevalence of hepatic steatosis in an urban population in the United States: impact of ethnicity. Hepatology. 2004; 40(6):1387–95. [PubMed: 15565570]
3. Adams LA, et al. The natural history of nonalcoholic fatty liver disease: A population-based cohort study. Gastroenterology. 2005; 129(1):113–121. [PubMed: 16012941]
4. Sanyal AJ, et al. Nonalcoholic steatohepatitis: association of insulin resistance and mitochondrial abnormalities. Gastroenterology. 2001; 120(5):1183–92. [PubMed: 11266382]
5. Kusminski CM, et al. Diabetes and apoptosis: lipotoxicity. Apoptosis. 2009; 14(12):1484–95. [PubMed: 19421860]
6. Unger RH, Orci L. Lipoapoptosis: its mechanism and its diseases. Biochim Biophys Acta. 2002; 1585(2–3):202–12. [PubMed: 12531555]
7. Feldstein AE, et al. Hepatocyte apoptosis and fas expression are prominent features of human nonalcoholic steatohepatitis. Gastroenterology. 2003; 125(2):437–43. [PubMed: 12891546]
8. Feldstein AE, et al. Cytokeratin-18 fragment levels as noninvasive biomarkers for nonalcoholic steatohepatitis: a multicenter validation study. Hepatology. 2009; 50(4):1072–8. [PubMed: 19585618]
9. Wei Y, et al. Saturated fatty acids induce endoplasmic reticulum stress and apoptosis independently of ceramide in liver cells. Am J Physiol Endocrinol Metab. 2006; 291(2):E275–81. [PubMed: 16492686]
10. Rutkowski DT, Kaufman RJ. A trip to the ER: coping with stress. Trends Cell Biol. 2004; 14(1): 20–8. [PubMed: 14729177]
11. Kaplowitz N, et al. Endoplasmic reticulum stress and liver injury. Semin Liver Dis. 2007; 27(4): 367–77. [PubMed: 17979073]
12. Rahman SM, et al. CCAAT/enhancing binding protein beta deletion in mice attenuates inflammation, endoplasmic reticulum stress, and lipid accumulation in diet-induced nonalcoholic steatohepatitis. Hepatology. 2007; 45(5):1108–17. [PubMed: 17464987]
13. Kaufman RJ. Orchestrating the unfolded protein response in health and disease. J Clin Invest. 2002; 110(10):1389–98. [PubMed: 12438434]
14. Malhi H, et al. Free fatty acids induce JNK-dependent hepatocyte lipoapoptosis. J Biol Chem. 2006; 281(17):12093–101. [PubMed: 16505490]
15. Puri P, et al. Activation and dysregulation of the unfolded protein response in nonalcoholic fatty liver disease. Gastroenterology. 2008; 134(2):568–76. [PubMed: 18082745]
16. Wang Y, et al. Increased apoptosis in high-fat diet-induced nonalcoholic steatohepatitis in rats is associated with c-Jun NH2-terminal kinase activation and elevated proapoptotic Bax. J Nutr. 2008; 138(10):1866–71. [PubMed: 18806094]
17. Singh R, et al. Differential effects of JNK1 and JNK2 inhibition on murine steatohepatitis and insulin resistance. Hepatology. 2009; 49(1):87–96. [PubMed: 19053047]
18. Cazanave SC, et al. JNK1-dependent PUMA expression contributes to hepatocyte lipoapoptosis. J Biol Chem. 2009; 284(39):26591–602. [PubMed: 19638343]
19. Dhanasekaran DN, Reddy EP. JNK signaling in apoptosis. Oncogene. 2008; 27(48):6245–51. [PubMed: 18931691]
20. Barreyro FJ, et al. Transcriptional regulation of Bim by FoxO3A mediates hepatocyte lipoapoptosis. J Biol Chem. 2007; 282(37):27141–54. [PubMed: 17626006]
21. Linseman DA, et al. Glycogen synthase kinase-3beta phosphorylates Bax and promotes its mitochondrial localization during neuronal apoptosis. J Neurosci. 2004; 24(44):9993–10002. [PubMed: 15525785]
22. Hongisto V, et al. Lithium blocks the c-Jun stress response and protects neurons via its action on glycogen synthase kinase 3. Mol Cell Biol. 2003; 23(17):6027–36. [PubMed: 12917327]

23. Maurer U, et al. Glycogen synthase kinase-3 regulates mitochondrial outer membrane permeabilization and apoptosis by destabilization of MCL-1. Mol Cell. 2006; 21(6):749–60. [PubMed: 16543145]
24. Shinohara M, et al. Silencing glycogen synthase kinase-3beta inhibits acetaminophen hepatotoxicity and attenuates JNK activation and loss of glutamate cysteine ligase and myeloid cell leukemia sequence 1. J Biol Chem. 285(11):8244–55. [PubMed: 20061376]
25. Eldar-Finkelman H. Glycogen synthase kinase 3: an emerging therapeutic target. Trends Mol Med. 2002; 8(3):126–32. [PubMed: 11879773]
26. Kim AJ, et al. Valproate protects cells from ER stress-induced lipid accumulation and apoptosis by inhibiting glycogen synthase kinase-3. J Cell Sci. 2005; 118(Pt 1):89–99. [PubMed: 15585578]
27. Bowes AJ, et al. Valproate attenuates accelerated atherosclerosis in hyperglycemic apoE-deficient mice: evidence in support of a role for endoplasmic reticulum stress and glycogen synthase kinase-3 in lesion development and hepatic steatosis. Am J Pathol. 2009; 174(1):330–42. [PubMed: 19095952]
28. Song L, De Sarno P, Jope RS. Central role of glycogen synthase kinase-3beta in endoplasmic reticulum stress-induced caspase-3 activation. J Biol Chem. 2002; 277(47):44701–8. [PubMed: 12228224]
29. Cross DA, et al. Selective small-molecule inhibitors of glycogen synthase kinase-3 activity protect primary neurones from death. J Neurochem. 2001; 77(1):94–102. [PubMed: 11279265]
30. Chuang DM, et al. Neuroprotective effects of lithium in cultured cells and animal models of diseases. Bipolar Disord. 2002; 4(2):129–36. [PubMed: 12071510]
31. Akazawa Y, et al. Palmitoleate attenuates palmitate-induced Bim and PUMA up-regulation and hepatocyte lipoapoptosis. J Hepatol. 52(4):586–93. [PubMed: 20206402]
32. Faubion WA, et al. Toxic bile salts induce rodent hepatocyte apoptosis via direct activation of Fas. J Clin Invest. 1999; 103(1):137–45. [PubMed: 9884343]
33. Richieri GV, Kleinfeld AM. Unbound free fatty acid levels in human serum. J Lipid Res. 1995; 36(2):229–40. [PubMed: 7751810]
34. Belfort R, et al. A placebo-controlled trial of pioglitazone in subjects with nonalcoholic steatohepatitis. N Engl J Med. 2006; 355(22):2297–307. [PubMed: 17135584]
35. Langer DA, et al. Nitric oxide promotes caspase-independent hepatic stellate cell apoptosis through the generation of reactive oxygen species. Hepatology. 2008; 47(6):1983–93. [PubMed: 18459124]
36. Sato N, et al. Maintenance of pluripotency in human and mouse embryonic stem cells through activation of Wnt signaling by a pharmacological GSK-3-specific inhibitor. Nat Med. 2004; 10(1): 55–63. [PubMed: 14702635]
37. Jian W, et al. Enzastaurin shows preclinical antitumor activity against human transitional cell carcinoma and enhances the activity of gemcitabine. Mol Cancer Ther. 2009; 8(7):1772–8. [PubMed: 19509273]
38. Hsu YT, Youle RJ. Nonionic detergents induce dimerization among members of the Bcl-2 family. J Biol Chem. 1997; 272(21):13829–34. [PubMed: 9153240]
39. Masuoka HC, et al. Mcl-1 degradation during hepatocyte lipoapoptosis. J Biol Chem. 2009; 284(44):30039–48. [PubMed: 19734538]
40. Hoeflich KP, et al. Requirement for glycogen synthase kinase-3beta in cell survival and NF-kappaB activation. Nature. 2000; 406(6791):86–90. [PubMed: 10894547]
41. Meijer L, Flajolet M, Greengard P. Pharmacological inhibitors of glycogen synthase kinase 3. Trends Pharmacol Sci. 2004; 25(9):471–80. [PubMed: 15559249]
42. Hongisto V, et al. The Wnt pool of glycogen synthase kinase 3beta is critical for trophic-deprivation-induced neuronal death. Mol Cell Biol. 2008; 28(5):1515–27. [PubMed: 18195042]
43. Mott DM, et al. Palmitate action to inhibit glycogen synthase and stimulate protein phosphatase 2A increases with risk factors for type 2 diabetes. Am J Physiol Endocrinol Metab. 2008; 294(2):E444–50. [PubMed: 18056794]
44. Mora A, et al. Lithium blocks the PKB and GSK3 dephosphorylation induced by ceramide through protein phosphatase-2A. Cell Signal. 2002; 14(6):557–62. [PubMed: 11897496]

45. Lin CF, et al. GSK-3beta acts downstream of PP2A and the PI 3-kinase-Akt pathway, and upstream of caspase-2 in ceramide-induced mitochondrial apoptosis. J Cell Sci. 2007; 120(Pt 16): 2935–43. [PubMed: 17666435]

46. Mishra R, et al. Glycogen synthase kinase-3beta induces neuronal cell death via direct phosphorylation of mixed lineage kinase 3. J Biol Chem. 2007; 282(42):30393–405. [PubMed: 17711861]

47. Kim JW, et al. Glycogen synthase kinase 3 beta is a natural activator of mitogen-activated protein kinase/extracellular signal-regulated kinase kinase kinase 1 (MEKK1). J Biol Chem. 2003; 278(16):13995–4001. [PubMed: 12584189]

48. Malhi H, Gores GJ. Cellular and molecular mechanisms of liver injury. Gastroenterology. 2008; 134(6):1641–54. [PubMed: 18471544]

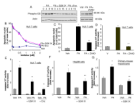

Figure 1. GSK-3 inhibition attenuates PA mediated apoptosis

(A) Whole cell lysates were prepared from Huh-7 cells treated with vehicle (Veh) or PA at 800 μM in the presence of the GSK-3 inhibitors, GSK IX or enzastaurin (Enz) (10 μM) for 4, 8 and 16 hours, or ZVAD (25 μM) for 16 hrs. Immunoblot analyses were performed for phosphorylated glycogen synthase (Phospho-GS) and β-actin was used as a control for protein loading. (B, C) Huh-7 cells were treated for 24 hours with Veh or PA at 800 μM in the presence of either an increasing concentrations of GSK IX or Enz up to 2 μM, or ZVAD (25 μM). Apoptosis was assessed by morphological criteria after DAPI staining. Data represents the mean ± SEM for three experiments. (D, E) Huh-7 cells were treated for 24 hours with Veh or PA at 800 μM in the presence of either GSK IX, Enz at 2 μM, or ZVAD (25 μM). (F) Hep3B cells (G) or mouse primary hepatocytes were treated for 16 hours with Veh or PA at 400 μM in the presence of GSK IX at 2 μM. (D, E, F and G) Caspase 3/7 catalytic activity was measured by a fluorogenic assay. Fold-increase was determined over control value (vehicle-treated cells), arbitrarily set to 1. Data represent the mean ± SEM for three experiments. $^{*}p < 0.05$, Veh-treated cells vs PA-treated cells; $^{**}p < 0.05$, PA-treated cells vs. PA plus GSK IX-treated cells or PA plus Enz-treated cells or PA plus ZVAD.

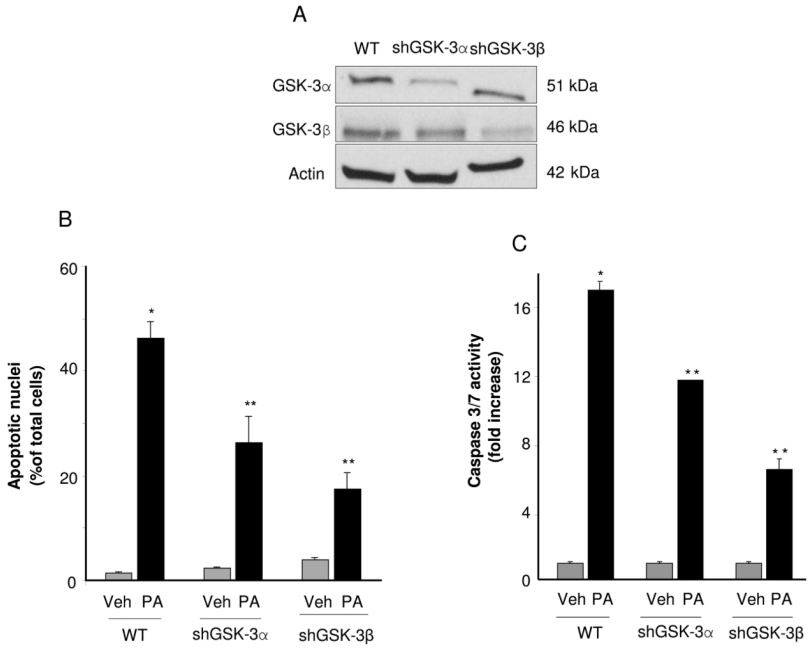

Figure 2. GSK-3α and GSK-3β targeted shRNA reduce PA-mediated lipotoxicity

Huh-7 Wild type (WT) or Huh-7 cells stably expressing short hairpin RNA targeting GSK-3α (shGSK-3α) or GSK-3β (shGSK-3β) were treated for 16 hours with Veh, or PA at 400 μM. (A) Effective and selective downregulation of GSK-3α or GSK-3β protein levels in shGSK-3α or shGSK-3β Huh-7 cells, respectively, compared to WT Huh-7 cells was verified by immunoblot analysis on whole cell lysates. (B) Apoptosis was assessed by morphological criteria after DAPI staining. (C) Caspase 3/7 catalytic activity was measured by the fluorogenic assay. Fold-increase was determined over control value (vehicle-treated cells), arbitrarily set to 1. $^{*}p < 0.05$, Veh-treated cells vs PA-treated cells; $^{**}p < 0.05$, PA-treated WT cells vs PA-treated shGSK-3α or shGSK-3β.

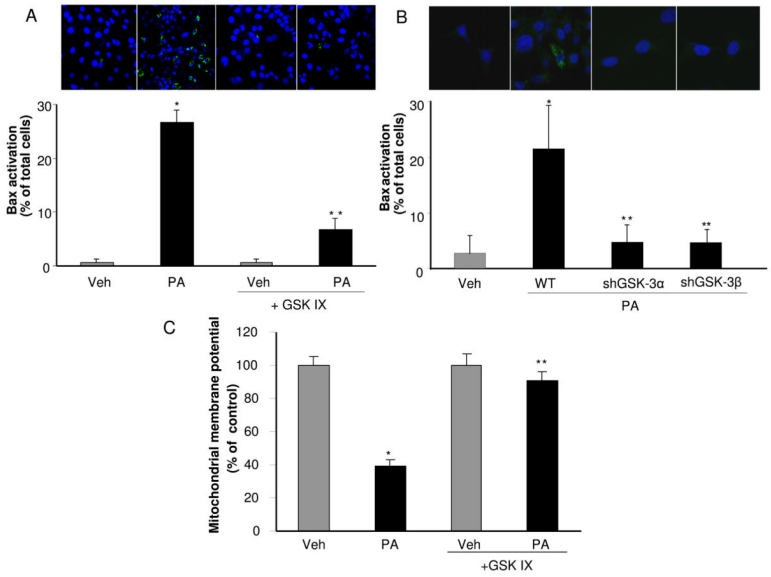

Figure 3. GSK-3 inhibition attenuates Bax activation and drop in MMP induced by PA

(A) Huh-7 cells were treated for 16 hours with Veh or PA at 800 μM in the presence of the GSK-3 inhibitor GSK IX at 2 μM. (B) WT Huh-7, shGSK-3α Huh-7 and shGSK-3β Huh-7 were treated for 16 hours with Veh, or PA at 400 μM. (A and B) Cells were fixed and Bax activation was assessed using conformation specific antisera (6A7) and immunofluorescence microscopy. Representative images of three independent experiments are depicted. Bax activation was quantified in 5 random 40 X objective field for each condition with automated software. (C) Huh-7 cells were treated for 16 hours with Veh or PA at 400 μM in the presence of the GSK-3 inhibitor GSK IX at 10 μM. Mitochondrial depolarization was measured using tetramethylrhodamine methylester. A minimum of 15 randomly selected cells were analyzed per condition from multiple microscopic fields. Data represents the mean ± SEM for three experiments. $^{*}p < 0.05$, Veh-treated cells vs PA-treated cells; $^{**}p < 0.01$, PA-treated cells vs PA plus GSK IX-treated cells or PA-treated WT cells vs. PA-treated shGSK-3α or shGSK-3β.

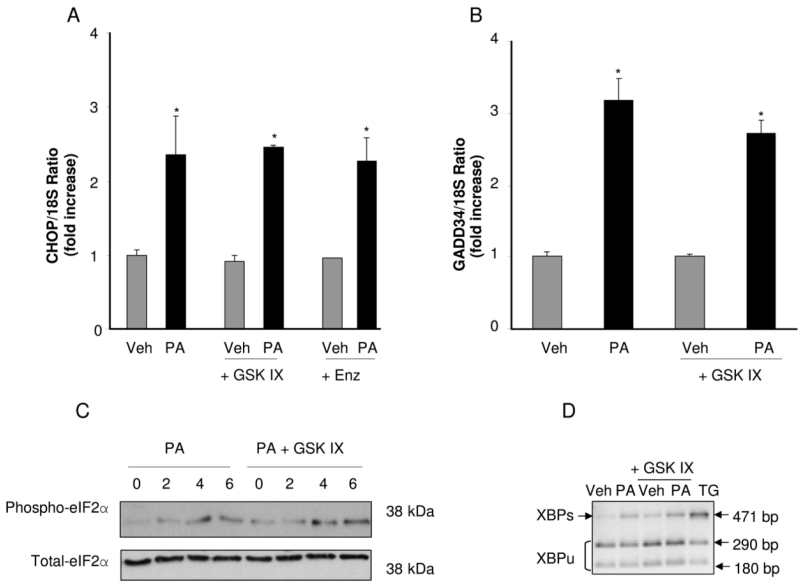

Figure 4. GSK-3 inhibition does not decrease PA-induced CHOP and GADD34 up-regulation, eIF2α phosphorylation or XBP-1 splicing

Huh-7 cells were treated with Veh or PA at 800 μM in the presence of the GSK-3 inhibitors GSK IX or Enz at 2 μM. (A and B) Total RNA was extracted 8 hours after treatments, and *CHOP* and *GADD34* mRNA were quantified by real-time PCR. Fold induction was determined after normalization to 18S. Data represent the mean ± SEM, of three independent experiments. $^{*}p < 0.05$, Veh-treated cells vs PA-treated cells. (C) Whole cell lysates were prepared 2, 4 and 6 hours after treatments. Immunoblot analyses were performed for phosphorylated eIF2α and total eIF2α was used as a control for protein loading. (D) *XBP-1* cDNA was amplified by PCR, followed by incubation with PstI. In Veh-treated cells, most XBP-1 PCR products were cut by PstI, producing 290 bp and 180 bp amplification products, indicative of native and unspliced form of *XBP-1* mRNA (XBP1u). A 471 bp amplification product, indicative of spliced *XBP-1* mRNA (XBP1s) was mainly observed in PA-treated cells. Thapsigargin (TG)-treated cells at 450 nM were used as a positive control for *XBP-1* mRNA splicing.

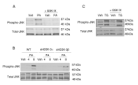

Figure 5. Pharmacological or genetic inhibition of GSK-3 reduces PA-induced activating JNK phosphorylation

Whole cell lysates were prepared from Huh-7 cells treated for 4 hours (A) with Veh or PA at 800 μM in presence of the pharmacological GSK-3 inhibitor GSK IX (2 μM), and (C) with Veh or thapsigargin (TG) (450 nM) in the presence of GSK IX (2 μM). (B) Whole cell lysate were prepared from WT Huh-7, shGSK-3α Huh-7 and shGSK-3β Huh-7 treated for 4 and 8 hours with Veh or PA at 800 μM. (A, B and C) Immunoblot analyses were performed for phosphorylated JNK; total JNK was used as a control for protein loading.

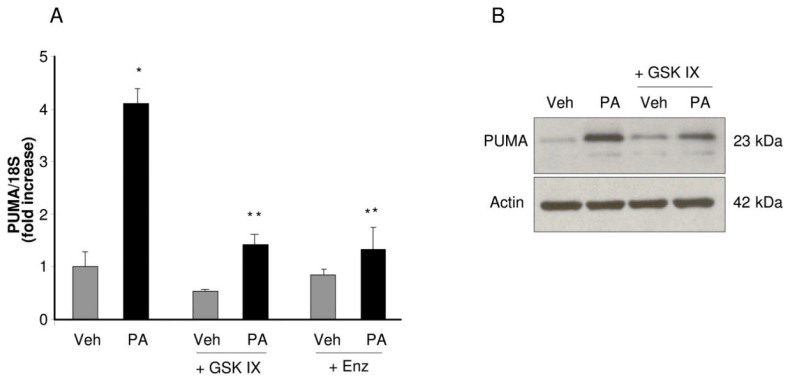

Figure 6. GSK-3 inhibitor suppresses PA-mediated PUMA upregulation

(A and B) Huh-7 cells were treated with Veh or PA at 800 μM in the presence of the GSK-3 inhibitors GSK IX or Enz at 2 μM. (A) Total RNA was extracted 8 hours after treatments and *PUMA* mRNA was quantified by real-time PCR. Fold induction was determined after normalization to 18S. Data represent the mean ± SEM, of three independent experiments. $^{*}p < 0.05$, Veh-treated cells vs PA-treated cells; $^{**}p < 0.05$, PA-treated cells vs. PA plus GSK IX or PA plus Enz-treated cells. (B) Whole cell lysates were prepared 16 hours after treatments and immunoblot analyses were performed for PUMA; β-actin was used as a control for protein loading.

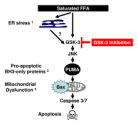

Figure 7. Proposed model for the effects of GSK-3 inhibition on PA-induced apoptosis

GSK-3 inhibition blocks JNK phosphorylation thereby preventing PUMA upregulation, Bax activation, and attenuates PA-induced cell death. [1] reference [9], [2] reference [18], [3] reference [14].